
This is an electronic reprint of the original article.
This reprint may differ from the original in pagination and typographic detail.

Han, Bing; Ezeanowi, Nnaemeka C.; Koironen, Tuomas O.; Häkkinen, Antti T.; Louhi-Kultanen, Marjatta

Insights into Design Criteria for a Continuous, Sonicated Modular Tubular Cooling Crystallizer

Published in:
Crystal Growth and Design

DOI:
[10.1021/acs.cgd.8b00700](https://doi.org/10.1021/acs.cgd.8b00700)

Published: 24/10/2018

Published under the following license:
Unspecified

Please cite the original version:
Han, B., Ezeanowi, N. C., Koironen, T. O., Häkkinen, A. T., & Louhi-Kultanen, M. (2018). Insights into Design Criteria for a Continuous, Sonicated Modular Tubular Cooling Crystallizer. *Crystal Growth and Design*, 18(12), 7286-7295. <https://doi.org/10.1021/acs.cgd.8b00700>

This material is protected by copyright and other intellectual property rights, and duplication or sale of all or part of any of the repository collections is not permitted, except that material may be duplicated by you for your research use or educational purposes in electronic or print form. You must obtain permission for any other use. Electronic or print copies may not be offered, whether for sale or otherwise to anyone who is not an authorised user.

19 Keywords: Continuous crystallization; Modular crystallizer; Tubular flow; Ultrasound

20

21 **1. INTRODUCTION**

22 When compared with batch or semi-batch crystallization process modes, continuous crystallization
23 has many advantages such as smaller volumes required, higher efficiency, higher product
24 reproducibility, less cost of labor and operation, and higher flexibility.^{1,2} All of these are considerably
25 important for obtaining reproducible and narrow crystal size distributions, uniform particles and specific
26 crystal morphologies. Various designs of continuous pipe crystallizers are nowadays getting much more
27 popular than the mixed-suspension mixed-product-removal crystallizers because crystal classification
28 effects can be minimized in the tubular reactor. Additionally, the scale up is much easier with
29 continuous plug flow crystallizer. However, Hohmann et al.³ have pointed out the problematics of
30 clogging and pipe blocking which can be minimized using seed generating systems.

31 One of the most popular continuous tubular flow crystallizer is the continuous oscillatory baffled
32 crystallizer (COBC).^{2,4} Uniform products can be achieved with plug flow by proper control of nucleation
33 and crystal growth rate. With the control of frequency and amplitude of the oscillation, particle
34 fluidization and a narrow residence time distribution can be achieved due to intensive macro-structure
35 tubular mixing. Meanwhile, the particle size is affected by the set-up and operational conditions.

36 NiTech® Solutions Limited⁵ developed these kinds of crystallizers with different size suitable for various
37 application such as chemical synthesis and crystallization. Kacker et al.⁶ investigated residence time
38 distribution of dispersed liquid and solid phase in a commercial COBC from NiTech Solutions® and
39 pointed out that operation at relative low amplitudes leads to optimal plug flow behavior.

40 To overcome the challenge of curve cooling in plug flow crystallization, Hohmann et al.³ designed a
41 continuous cooling crystallization on lab scale by applying the concept of a coiled flow inverter (CFI)
42 based on blended helically coiled tubes. Linear cooling or curve cooling employed with counter-current

43 air cooling can be operated with this device. Recently, Hohmann et al.⁷ also analyzed the effect of crystal
44 size dispersion in the designed tubular crystallizer by experiments and modeling and found that crystal
45 growth and growth rate dispersion were both dominating the product size distribution. A narrow
46 product size distribution can be obtained and revealed by simulation when using CFI crystallizer in
47 homogeneous suspension flow regime. Small volume mean diameters due to decreased tendency of
48 agglomeration and reduced time for crystal growth can be obtained at higher flow velocities⁸. On the
49 other hand, a clear fact is that crystal size decreases as sonication time increases.⁹ In ultrasound assisted
50 continuous tubular reactors sonication is manipulated by changing residence time.

51 Ultrasound has been used in many areas including medical diagnostics, thermoplastic welding,
52 cleaning of surfaces, wastewater treatment and food industry.¹⁰ It has also been employed in new fields
53 such as preparation of amorphous and nanostructured materials.^{11,12} Recently, the use of
54 sonocrystallization, that is crystallization assisted by ultrasound, in pharmaceutical and fine chemical
55 industry has attracted more interest of researchers because of the viability of this technology. In
56 addition, Zhang et al.¹³ had earlier reviewed the progress of continuous crystallization in
57 pharmaceuticals. Sonocrystallization is considered as an easy to use and easy to control technique, and
58 the end product with target crystal size, shape and polymorphs can be obtained.¹⁴ That is because the
59 metastable zone width (MZW) can be narrowed by introducing ultrasound, and ultrasound can disrupt
60 the formed crystal aggregates.¹ Furthermore, the effects of ultrasound on crystal growth was
61 theoretically studied in literature¹⁵ and was pointed out that the growth rate depends on the magnitude
62 of the supersaturation driving force. Arakelyan¹⁵ also highlighted that the crystal growth rate can be
63 doubled at low supersaturation by ultrasound, whereas there is no remarkable effect at high
64 supersaturation. Induction time can also be affected by ultrasound, as induction time decreases with
65 increase in ultrasound power.¹⁶ Besides these, the use of ultrasound can not only reduce the
66 crystallization time but can also offer a clean and efficient tool to improve the existing process.

67 Some studies have demonstrated that the use of ultrasound can drastically reduce fouling in
68 microchannel heat exchangers because of flow changes of the particle suspensions.¹⁷⁻²⁰ As proposed by
69 Rossi et al.,¹⁹ transient cavitation of bubbles induced by sonication played a significant role for
70 promoting nucleation with observations from the experiments and numerical simulations. Recently, a
71 sonicated tubular crystallization system, to control particle size without clogging, was successfully
72 designed and specified for an active pharmaceutical ingredient (API) compound.²¹ In addition, a
73 crystallizer cascade can offer economic advantages over a single-body crystallizer of the same volume.²²
74 Several continuous MSMPR multistage cooling crystallizers have been reported in literature.²³⁻²⁵
75 Furthermore, Siddique et al.²⁶ successfully applied sonication to initialize crystallization in COBC without
76 fouling or agglomeration issues for lactose. However, the yield was relatively low compared to when
77 operated with a sonicated batch crystallizer due to insufficient seeds produced by limited ultrasound
78 power. Continuous sonocrystallization of acetylsalicylic acid in a tubular crystallizer with multiple cooling
79 sections has been investigated in literatures.^{27,28} Ultrasound was used at the initial period to generate
80 seed crystals before multiple cooling stages in their system.

81 Lawton et al.² have demonstrated continuous plug flow crystallizer operation with oscillatory baffled
82 reactor (OBR), and Ruecroft & Burns²⁹ have made patent application combining ultrasound and pipe
83 modules for antisolvent crystallization. This is different from the current research work where
84 ultrasound is applied continuously to each cooling stage. To our best knowledge, the cooling strategies
85 of continuous tubular flow crystallization integrated with ultrasound have not been studied widely.
86 Therefore, in the present work the ultrasound technology and continuous modular crystallization are
87 combined to investigate operational availability of the whole process and crystal properties with
88 different selected model compounds in order to design a tubular crystallizer for a specific application. It
89 is expected to overcome the challenges of channel clogging and suspension pumping with ultrasound in
90 the designed continuous tubular flow crystallizer. Three model compounds comprising of inorganic and

91 organic substances were selected to investigate the design criteria for the ultrasonically assisted
92 crystallizer concerning cooling crystallization.

93

94 **2. EXPERIMENTAL SECTION**

95 **2.1 Materials**

96 Three model compounds, K_2SO_4 (≥ 99 % purity), $CuSO_4$ (100 % purity) and phthalic acid (99 % purity)
97 with analytical grade, were used in the crystallization experiments of the present work. Deionized water
98 was used as the solvent for all the compounds.

99

100 **2.2 Experimental set-up and method**

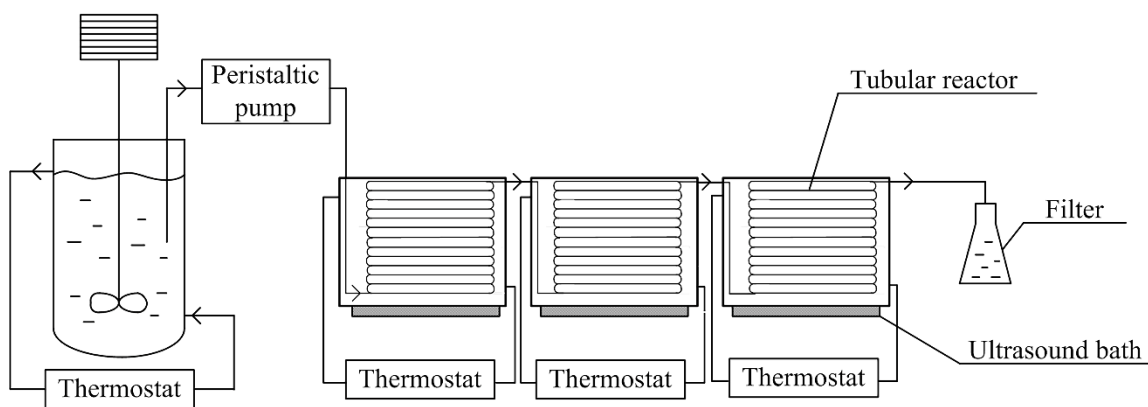
101 The experimental set-up shown in Figure 1 consisted of a stirred feed tank, a peristaltic pump
102 (Masterflex Pump Easy Load II 77201-62), three modular crystallizers separately immersed into three
103 ultrasound baths (Bandelin sonorex digitec DT102H, 35 kHz) equipped with thermostats (Lauda), and a
104 collection unit. The feed tank was a jacketed glass reactor with a capacity of 4.5 L equipped with a
105 pitched blade turbine impeller and a thermostat (Lauda). A modular crystallizer was made from a
106 spiraled EN 1.4307 / AISI 304 L stainless steel pipe, which was 12 m or 18 m in length (depending on the
107 experiment), had an inner diameter of 4 mm and 1 mm wall thickness. No polishing was done to the
108 inner walls of the pipe. Each 12 m stainless steel pipe was wound in an oval shape of 14 cm in length and
109 9.5 cm in width, whereas the 18m stainless steel pipes were wound in an oval shape of 17.5 cm in length
110 and 10.5 cm in width. The wound pipes were placed into a 3L ultrasound bath for each module. Three
111 modules with same configuration were installed in series.

112 A certain amount of saturated solution was firstly prepared in the feed tank at temperature which was
113 5.0 °C higher than the equilibrium temperature of the saturated solution in order to dissolve all the
114 solids at the beginning. The temperature of the feed solution was controlled by a thermostat. Different

115 temperatures were set at each modular tubular crystallizer according to the designed cooling strategy.
116 The final outlet temperature of the crystallized solution was fixed at 20.0 °C. Before the experiment,
117 thermostats and ultrasound baths were started to keep the temperature and ultrasound power steady
118 in the modular crystallizers. The feed solution was pumped by a peristaltic pump to the first, second and
119 third modular tubular crystallizers serially. If the process can be operated without clogging for three or
120 more times of residence time, then it was defined as a feasible operating condition.

121 Finally, the suspensions were filtered with a vacuum filter and the crystals were dried in an oven.
122 Morphology and crystal size of the solids obtained from cooling crystallization were analyzed by an
123 automatic image analyzer (Malvern Morphologi G3). About 75000 product crystals were analyzed for
124 each experiment. The crystal yield was calculated from the total mass of the crystals obtained at the end
125 of the experiments.

126



127

128 **Figure 1.** Flow diagram of the modular continuous crystallization system

129

130 **2.3 Effect of Residence time**

131 The residence time of the solution in the crystallizer is an important factor in continuous
132 crystallization and it is determined by the set flow rate. Furthermore, the flow velocity should be high
133 enough to avoid settling of crystals in the tube and still suitable to experience enough residence time for

134 crystallization in the system. The Reynolds number (Re) for the flow in the crystallizer were in the range
 135 of 260 – 1300. Hence, all the flow rates used in the experiment provided laminar flow in the tube. In
 136 order to get test runs of feasible operating conditions, various flow rates were firstly investigated with
 137 model compounds K_2SO_4 and $CuSO_4$. These preliminary experiments were carried out with pipes that
 138 were 12 m in length and had 4 mm inner diameter and 1 mm wall thickness. Table 1 shows the flow
 139 rates, their corresponding residence times and flow velocities in the pipe used in the current study.

140

141 **Table 1.** Flow rates, residence times and flow velocities in the modular crystallizer.

Flow rate Q, ml/min	Residence time τ , min	Flow velocity in the pipe v_f , cm/s
49	9.23	6.50
60	7.54	7.96
75	6.03	9.95
100	4.52	13.26
120	3.77	15.92

142

143 **2.4 Effect of cooling strategy**

144 The present study used modular tubular crystallizers in continuous cooling crystallization that enabled
 145 the supersaturation to be easily and accurately controlled. Control strategy plays a critical role to
 146 achieve feasible operating conditions,³⁰ as employed in the current system. Three cooling strategies
 147 which were equal concentration difference (equal supersaturation), equal temperature difference and
 148 equal supersaturation ratio were used. The cooling temperature profile for each experiment was
 149 calculated on the basis of the selected cooling strategy, and calculated temperatures are maintained for
 150 each module

151 Due to the results from the initial experiments regarding the influence of residence time, the flow
 152 rate of 75 ml/min as an optimal condition was used to study the cooling strategy. In addition, the length
 153 of the steel pipe in each module was increased to 18 m to accommodate longer residence times. Other

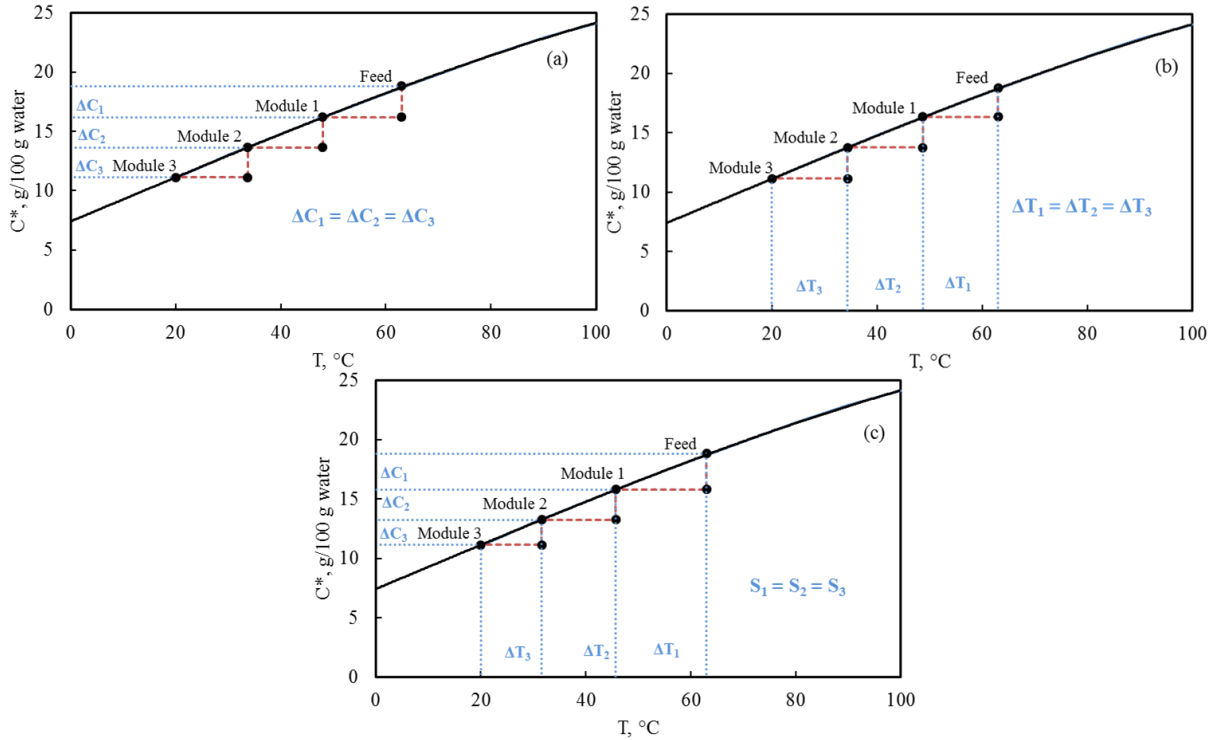
154 dimensions such as pipe diameter and thickness were kept the same. Thus, in order to keep a constant
155 production rate because the residence times changes with the longer pipes, the initial concentration of
156 model compounds used in the 18 m pipe was calculated in relation to the conditions used in 12 m pipe.

157

158 2.4.1 Supersaturation (ΔC)

159 The equal concentration difference in the three modules was initially considered. It ensures each module
160 or crystallization stage to reach the same supersaturation as shown in Figure 2a, Figure 3a, and Figure 4a
161 for the different model compounds. Since there were three modules in these set of experiments, the
162 supersaturation (ΔC) was shared equally to each module by calculation from the initial and final
163 concentrations based on the solubility curve. The corresponding temperatures of the resulting
164 concentrations were then used to set the cooling temperature profile.

165



166

167 **Figure 2.** Solubility curve of K_2SO_4 showing equal supersaturation (a), equal temperature difference (b),

168 and equal supersaturation ratio (c) in each module in a temperature range from 63.0 °C – 20.0 °C

169 (adapted from *docbrown.info*³¹).

170

171 2.4.2 Temperature difference (ΔT)

172 Mersmann and Rennie²² introduced a continuous multistage cooling crystallization process involving

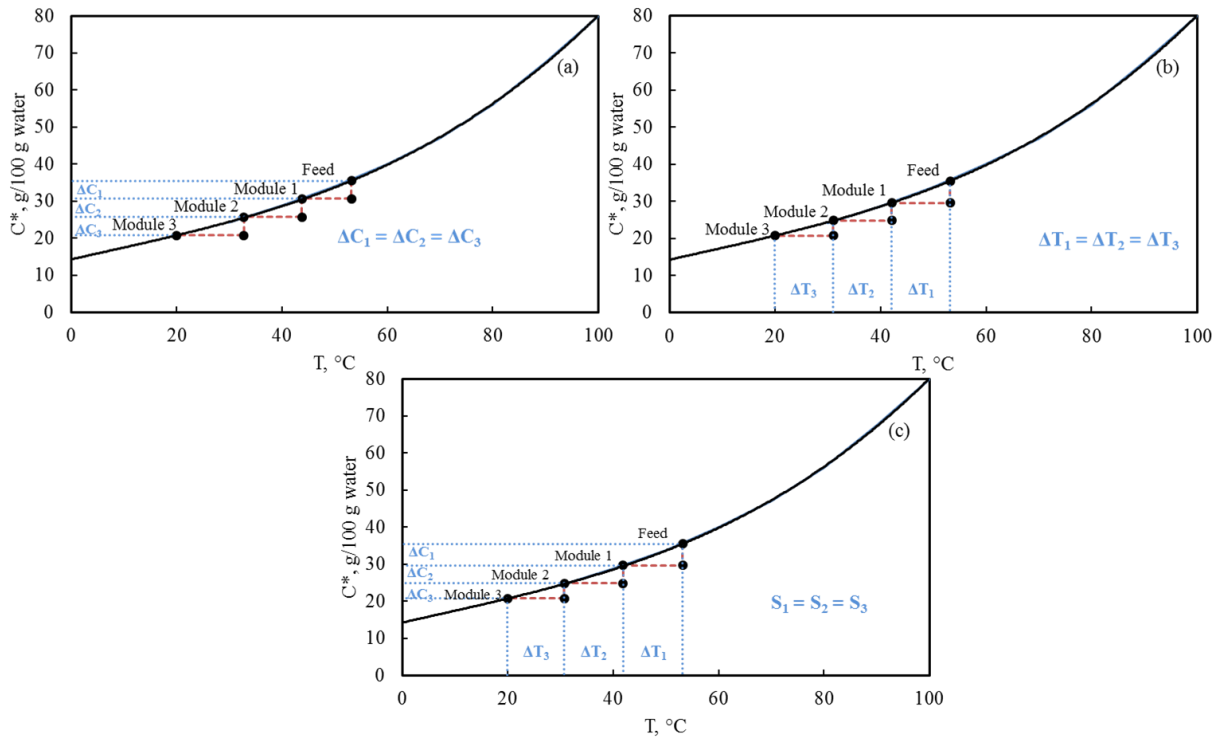
173 eight countercurrent crystallizers in series. This concept can help to avoid excess local supersaturation in

174 each stage. It means that the temperature drop should be equal in each module as shown in Figure 2b,

175 Figure 3b, and Figure 4b for the different model compounds. In this case, the concentration difference in

176 each module varies and it depends on the solubility of the model compound.

177



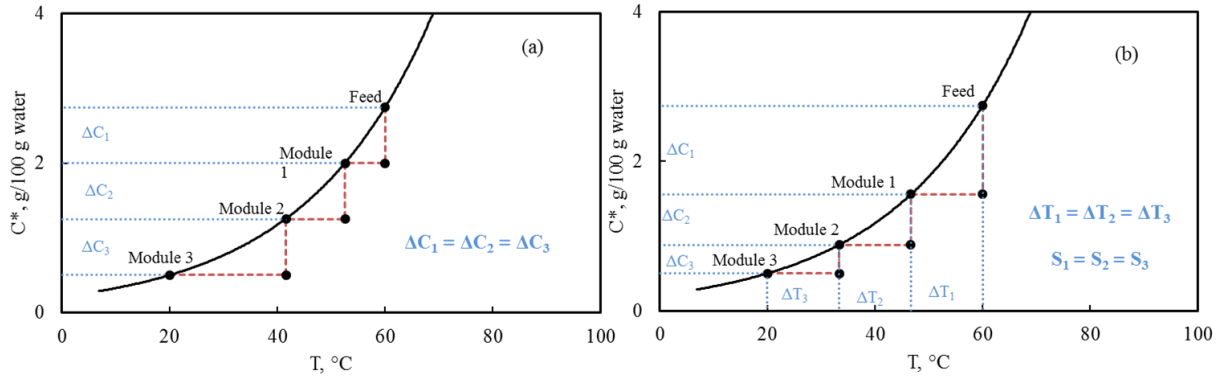
178
 179 **Figure 3.** Solubility curve of CuSO_4 showing equal supersaturation (a), equal temperature difference (b),
 180 and equal supersaturation ratio (c) in each module in a temperature range from $53.2\text{ }^\circ\text{C} - 20.0\text{ }^\circ\text{C}$
 181 (adapted from *docbrown.info*³¹).

182

183 2.4.3 Supersaturation ratio (S)

184 Supersaturation ratio ($S=C/C^*$) is another way to express supersaturation level in the system. The
 185 supersaturation ratio is calculated as the ratio of the initial concentration and expected final
 186 concentration at the exit of the module based on the solubility curve of the model compound. Thus,
 187 equal supersaturation ratio in each module was taken into account as a design method. In this case, the
 188 concentration difference decreases gradually with the modules, which can be clearly seen in Figure 2c,
 189 Figure 3c, Figure 4b and Table 2 for the different model compounds.

190



191
 192 **Figure 4.** Solubility curve of phthalic acid having equal supersaturation (a), equal temperature difference
 193 and equal supersaturation ratio (b), in each module in a temperature range from 60.0 °C – 20.0 °C
 194 (adapted from Stephen and Stephen³²).

195

196 2.5 Effect of supersaturation ratio

197 To understand the influence of supersaturation ratio on crystallization more deeply, various
 198 experiments with phthalic acid with different supersaturation ratios in the range from 1.20 to 1.90, as
 199 shown in Table 3, were performed with 3-stage modular crystallizer. Same experimental procedure as
 200 shown in section 2.2 was used with the same residence time of 9.05 min in every experiment. Crystal
 201 size distributions were examined with Morphologi G3.

202

203 2.6 Effect of ultrasound

204 Effect of ultrasound was investigated with phthalic acid for the studied continuous crystallizer. Two
 205 steel pipes having lengths of 12 m and 18 m were used. Same configuration but only one module which
 206 had spiraled pipes was considered here for cooling crystallization of phthalic acid in the temperature
 207 range from 35.0 °C to 20.0 °C. 3 liters of feed solution saturated at 35.0 °C was first prepared. The
 208 temperature of the thermostat used for the tubular crystallizer was set to 20.0 °C. Seeding was done in
 209 coherence with Linga's³³ recommendation for seeding in industrial crystallizers. Hence, 0.2 g (about

210 0.3 % of final crystals) seeds with average size of 11 μm was added to the saturated solution to initiate
211 crystallization. Five flow rates were used for the cooling crystallization processes of phthalic acid with
212 ultrasound while three flow rates were used for the experiments without ultrasound. In this case, the
213 product crystals were analyzed with Malvern Size Analyzer (Mastersizer 3000) to determine the particle
214 size distributions. Clear filtrates were weighed and dried in the oven to determine the concentration of
215 the soluble materials in the mother liquor. This method was used for crystal yield determination.

216

217 **3. RESULTS AND DISCUSSION**

218 **3.1 Effect of residence time**

219 *Potassium sulphate*. Various residence times shown in Table 1 were checked for K_2SO_4 with equal
220 concentration difference (1.63 g/100g water) in the range of 46.8 °C to 20.0 °C. The corresponding
221 supersaturation ratios in modules 1, 2 and 3 were 1.11, 1.13 and 1.15, respectively. The experimental
222 results show that the system was blocked when operated with a residence time of 9.23 mins. All the
223 other flow rates could offer feasible operations with the continuous modular crystallizer, their yield and
224 average particle sizes are presented in **Figure 5**. The reason for the blockage might be the existence of
225 excessive supersaturation in the module and low flow velocity, which is also pointed out by Furuta et
226 al.²¹ Crystal yield relates to the supersaturation level of the whole cooling process. It means that the
227 yield could be increased by increasing the initial concentration. Thus, two other experiments were
228 carried out with higher initial concentration corresponding to a temperature of 60.0 °C, at residence
229 times of 9.23 and 3.77 mins, to verify if a feasible operating condition could be achieved. Hence, a
230 feasible operating condition was observed with the residence time of 3.77 mins. Whereas, a blockage
231 occurred with the residence time of 9.23 mins due to the presence of excessive supersaturation in the
232 module and low flow velocity. Furuta et al.²¹ also reported same reason for blockages in their tubular
233 crystallizer.

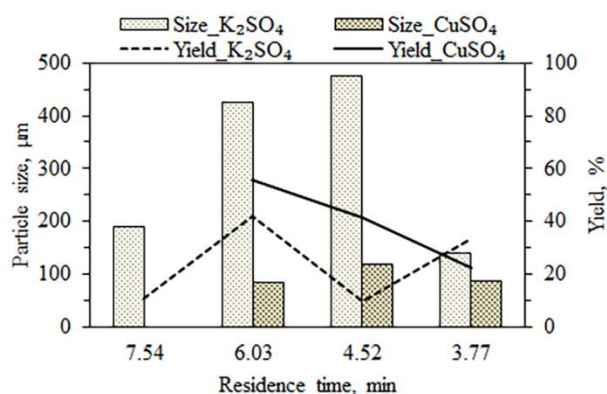
234 *Copper sulphate*. Due to the blockage which occurred in the continuous crystallization of K_2SO_4 with
235 the residence time of 9.23 mins, this residence time was not considered for $CuSO_4$ crystallization. Same
236 cooling profile with equal concentration difference was firstly employed with cooling crystallization of
237 $CuSO_4$ since feasible operating conditions were achieved while using the cooling strategy in K_2SO_4
238 crystallization. However, the blockage occurred for trial runs carried out with residence times of 7.54,
239 6.03 and 3.77 mins with equal concentration difference of 4.10, 4.77 and 6.43 g/100g water
240 corresponding to the initial temperatures 49.2, 53.0 and 60.0 °C, respectively. Because of this, equal
241 supersaturation ratio was considered with the same initial temperatures and flow rates, but there was
242 not any operation that led to a feasible operating condition. As Figure 2 and Figure 3 show, the solubility
243 of $CuSO_4$ in water is much higher than the solubility of K_2SO_4 , and the solubility curve of $CuSO_4$ is more
244 non-linear. Hence, sudden temperature decrease in the module leads to high supersaturation and thus
245 results in clogging of the crystallizer. Due to the aforementioned reasons, the initial temperature should
246 be decreased to achieve lower supersaturation level. Finally, three feasible operating conditions were
247 observed from experiments carried out with residence times of 6.03, 4.52 and 3.77 mins in the
248 temperature range from 43.0 to 20.0 °C by applying the cooling strategy of equal supersaturation ratio
249 (1.13).

250 Figure 5 shows the average crystal sizes ($D[4,3]$) based on volume distribution of different samples
251 obtained from feasible operating conditions of various residence times and yields for both compounds,
252 K_2SO_4 and $CuSO_4$. The crystal size of K_2SO_4 was always bigger than the size of $CuSO_4$ - crystals. This may
253 be due to the differences in crystal properties that drive the nucleation and growth. For both
254 compounds, the crystal size increased with the decrease of residence time and then reduced at shortest
255 residence time. Raphael et al.³⁴ observed that average crystal sizes decreases with shorter residence
256 times and was in line with results from Lawton et al.², whereas Rucroft et al.¹⁰ reported that with

257 continuous sonication smaller crystals are formed with longer residence times. Hence, the reason for
258 the variation in average crystal sizes might be the combined effect of ultrasound and residence time.

259 Furthermore, higher yield was obtained with the residence time of 6.03 mins, equivalent to a flow
260 rate of 75 ml/min, for both compounds as shown in Figure 5. It indicates that the flow rate of 75 ml/min
261 for the 3 stage reactor gave better results for the both model compounds. Therefore, this flow rate was
262 used to investigate cooling strategy of the modular crystallizer shown in section 3.2.

263



264

265 **Figure 5.** Crystal sizes of different samples obtained from feasible operating conditions of various
266 residence times and yields for both compounds K₂SO₄ and CuSO₄.

267

268 3.2 Effect of cooling strategy

269 Due to the increase of pipe length, the residence time was 9.05 mins when flow rate 75 ml/min was
270 used. In order to keep constant production rate after increasing the pipe length, the initial temperatures
271 used in the new configuration which was scaled up based on the observed feasible conditions obtained
272 from section 3.1 for K₂SO₄ and CuSO₄ were 63.0 °C and 53.2°C, respectively. Based on these parameters,
273 supersaturation, supersaturation ratio and temperature in each module were calculated as shown in
274 Table 2 and used for comparison of investigated cooling strategies.

275 *Potassium sulphate.* Feasible operating conditions were obtained with the design method of equal
276 concentration difference and equal temperature difference from continuous cooling crystallization of
277 K_2SO_4 , but the experiments designed by equal supersaturation ratio (S) failed. As shown in Table 2, the
278 first module had much higher supersaturation (ΔC) than module 2 and 3 when equal supersaturation
279 ratio (S) was used. It also indicates that equal supersaturation ratio provided faster cooling rates in the
280 first module compared with the other two methods which led to crash nucleation. Hartel³⁵ reported that
281 rapid cooling can cause the formation of higher amount of nuclei and high supersaturation can lead to
282 encrustation. Those may be the main reasons for clogging with the equal supersaturation ratio cooling
283 strategy. Crystal size distribution of K_2SO_4 with different cooling conditions are presented in Figure 6a. It
284 can be seen that larger crystals were obtained from the conditions with equal supersaturation (ΔC)
285 compared to equal temperature difference.

286 *Copper sulphate.* Continuous cooling crystallization of $CuSO_4$ in the continuous pipe were carried out
287 with the three designed cooling strategies in the temperature range from 53.2 °C to 20.0 °C. Figure 6b
288 shows the crystal size distribution of $CuSO_4$ obtained from continuous sonicated crystallization with
289 different cooling strategies. It shows that crystals were largest with equal temperature difference. Then,
290 slightly bigger particles were crystallized from equal supersaturation ratio (S) than with equal
291 supersaturation (ΔC).

292 *Phthalic acid.* An organic compound, phthalic acid, was selected to be used in the modular reactor. In
293 temperature range from 60.0 °C to 20.0 °C, continuous cooling crystallization experiments of phthalic
294 acid in the tubular crystallizer offered feasible operating conditions with three different cooling
295 strategies. As shown in Table 2, equal supersaturation ratio provides the same cooling profile with equal
296 temperature difference due to its solubility curve (adapted from Stephen & Stephen³²) shown in Figure
297 4. The crystal size distributions of phthalic acid obtained by various cooling conditions are shown in
298 Figure 6c. As can be seen, there are no significant differences in crystal sizes between equal

299 supersaturation and equal temperature difference (or equal supersaturation ratio). However,
 300 agglomerates are observed in **Figure 6c** since the CSDs were analyzed using the Morphologi G3 which
 301 measures crystal sizes by surface imaging. The potential reason for the agglomeration, hence the
 302 uneven CSDs, is that the supersaturation step in the last module is larger with equal temperature
 303 difference compared to equal supersaturation.

304

305

306

307

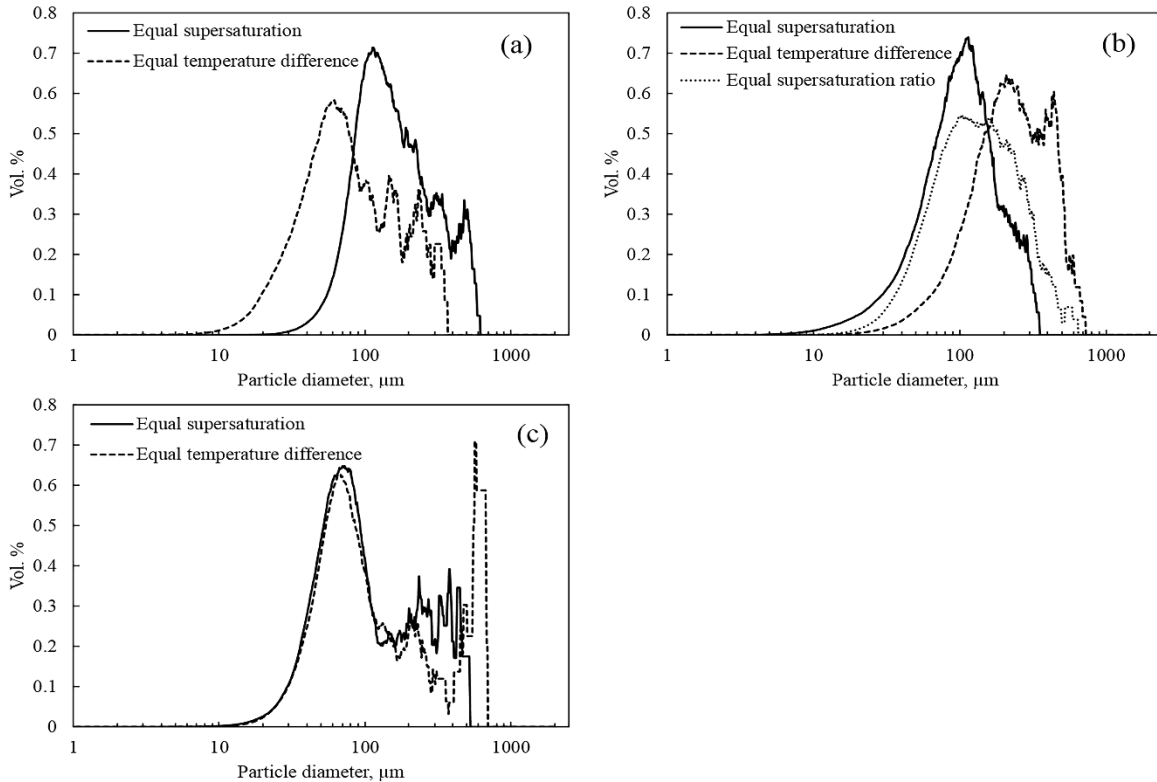
308 **Table 2.** Investigated cooling strategies for modular cooling crystallization with the residence time of
 309 9.05 mins and the obtained product yields of the model compounds.

Compound	Equal Condition	Unit	Conc., g/100g H ₂ O	ΔC , g/100g H ₂ O	S	ΔT , °C	Equivalent temp, °C	Yield ^a , %
K ₂ SO ₄	ΔC	Feed	18.73				63.0	24
		Module 1	16.20	2.54	1.16	15.05	48.0	
		Module 2	13.66	2.54	1.19	14.21	33.7	
		Module 3	11.12	2.54	1.23	13.75	20.0	
	ΔT	Feed	18.73				63.0	11
		Module 1	16.32	2.41	1.15	14.34	48.7	
		Module 2	13.77	2.55	1.19	14.34	34.3	
		Module 3	11.12	2.65	1.24	14.34	20.0	
	S	Feed	18.73				63.0	<i>Not a feasible operating condition</i>
		Module 1	15.74	2.99	1.19	17.63	45.4	
		Module 2	13.23	2.51	1.19	13.96	31.4	
		Module 3	11.12	2.11	1.19	11.42	20.0	

		Feed	35.13			53.2	
	ΔC	Module 1	30.32	4.81	1.16	9.52	43.7
		Module 2	25.51	4.81	1.19	10.99	32.7
		Module 3	20.70	4.81	1.23	12.65	20.0
		Feed	35.13			53.2	
CuSO ₄	ΔT	Module 1	29.60	5.52	1.19	11.05	42.2
		Module 2	24.86	4.74	1.19	11.05	31.1
		Module 3	20.70	4.16	1.20	11.05	20.0
		Feed	35.13			53.2	
	S	Module 1	29.45	5.68	1.19	11.39	41.8
		Module 2	24.69	4.76	1.19	11.15	30.7
		Module 3	20.70	3.99	1.19	10.62	20.0
		Feed	2.74			60.0	
	ΔC	Module 1	1.99	0.75	1.38	7.47	52.5
		Module 2	1.24	0.75	1.60	11.03	41.5
		Module 3	0.50	0.75	2.51	21.55	20.0
Phthalic acid	S / ΔT	Module 1	1.55	1.19	1.77	13.35	46.7
		Module 2	0.88	0.67	1.77	13.35	33.3
		Module 3	0.50	0.38	1.77	13.35	20.0

310 a = yield calculated from recovered dry product crystals, x = filter cloth torn during recovery

311



312
 313 **Figure 6.** Crystal size distribution of K₂SO₄ (a), CuSO₄ (b) and phthalic acid (c) crystallized by applying
 314 different cooling operating conditions at constant residence time of 9.05 mins in the continuous
 315 sonicated reactor.

316
 317 As a summary, almost all the model compounds crystallized from different cooling profiles in the
 318 continuous sonicated cooling crystallization process with a constant residence time achieved the highest
 319 yield when equal supersaturation was chosen as is shown in Table 2. Although, equal supersaturation
 320 ratio gave the highest actual yield for CuSO₄ but the actual yield was in the same range with that was
 321 obtained with equal supersaturation. It indicates that the supersaturation in each module is equally
 322 constant and this implies that the supersaturation in each crystallizer can be controlled accurately. This is
 323 consistent with the recommendation that was pointed out by Mersmann and Rennie.²² They suggested
 324 that cooling rates could be fixed by constant supersaturation in the cooling period. Therefore, equal

325 supersaturation between modules is the optimal cooling strategy in the modular crystallizer. However,
326 there are no clear trends corresponding to crystal size distributions probably because the kinetics and
327 crystal properties of different compounds are different. An additional reason may also be the impact of
328 ultrasound as there are possibilities of the crystals to observe a growth – attrition – growth sequence. It
329 means that crystal size can increase or decrease due to ultrasound because the induction of ultrasound
330 at different stages have different effects on crystals.^{14,36} Further studies of induction times are needed.

331

332 **3.3 Effect of supersaturation ratio**

333 Different initial temperatures were used to achieve different supersaturation ratios for phthalic acid
334 cooling crystallization at equal ΔS in each module as shown in Table 3. Continuous cooling crystallization
335 experiment of phthalic acid with equal supersaturation ratio of 1.20 did not result in crystal production.
336 This may be due to the extremely low supersaturation of the whole process. The experiment with
337 supersaturation ratio of 1.90 failed due to blockage problems, which were most probably caused by too
338 high supersaturation and faster cooling rate in the first module which led to encrustation and high
339 nucleation rate.^{35,37} Finally, there was blockage in the crystallizer. However, the continuous experiments
340 with other supersaturation ratios could be carried out without blockage.

341 The crystal size distributions and average crystal sizes of phthalic acid obtained from the feasible
342 operating conditions are presented in Figure 7. It shows that the crystal size distribution is getting
343 narrower with the increase of supersaturation ratio as presented in **Figure 7a** and the average crystal
344 size (D[4,3]) decreases with increase in equal supersaturation ratio as shown in **Figure 7b**. It can be
345 attributed to the effect of ultrasound and the supersaturation level in the first module which increased
346 with the increase of supersaturation ratio and thus lead to generation of small nuclei which provided
347 much more interface for crystal growth. Although Ni & Liao³⁸ and Kaneko et al.³⁹ reported that bigger
348 crystals are produced with higher supersaturation, however, the inverse relationship of the average

349 crystal size and supersaturation ratio is coherent with production of smaller crystals at high
 350 supersaturation as reported by Sarig et al.⁴⁰ The yield as shown in Table 3 indicates that the highest yield
 351 was obtained with the supersaturation ratio of 1.54 with the residence time of 9.05 mins which might be
 352 the optimal condition for this specific residence time.

353

354

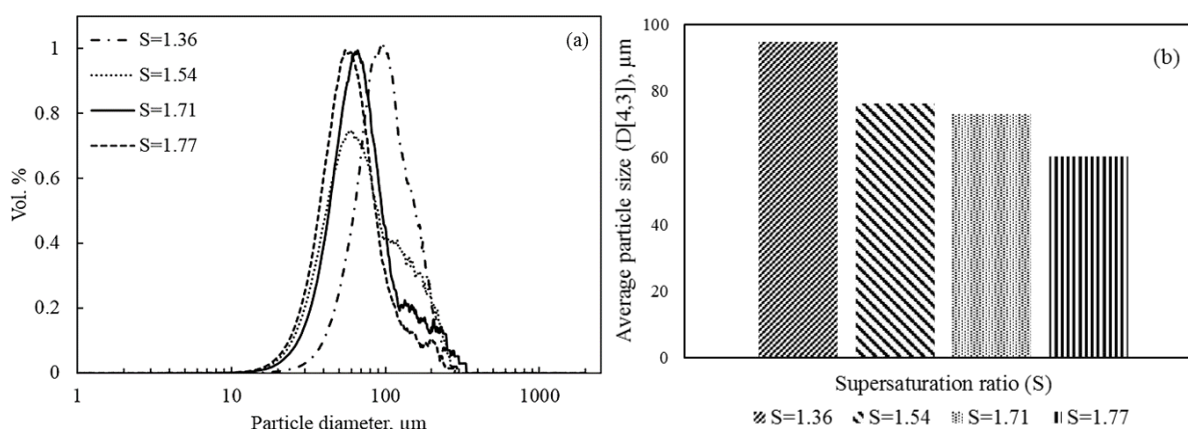
355 **Table 3.** The saturation concentrations of phthalic acid at equilibrium for each module and equivalent
 356 temperatures showing equal module supersaturation ratios.

Unit	C*, g/100 g H ₂ O	S	ΔC, g/100 g H ₂ O	Saturation temp., °C	Yield ^a , %
Feed	0.86			32.8	
Module 1	0.72	1.20	0.14	28.5	<i>no crystals</i>
Module 2	0.60	1.20	0.11	24.2	
Module 3	0.50	1.20	0.10	20.0	
Feed	1.24			41.4	
Module 1	0.91	1.36	0.33	34.3	24
Module 2	0.67	1.36	0.24	27.1	
Module 3	0.50	1.36	0.17	20.0	
Feed	1.80			50.2	
Module 1	1.17	1.54	0.63	40.1	59
Module 2	0.76	1.54	0.41	30.0	
Module 3	0.50	1.54	0.26	20.0	
Feed	2.50			57.8	
Module 1	1.46	1.71	1.04	45.2	39
Module 2	0.85	1.71	0.61	32.6	
Module 3	0.50	1.71	0.35	20.0	

Feed	2.74			60.0	
Module 1	1.55	1.77	1.19	46.7	39
Module 2	0.88	1.77	0.67	33.3	
Module 3	0.50	1.77	0.38	20.0	
Feed	3.39			65.0	
Module 1	1.79	1.90	1.60	50.0	<i>Not a feasible operating condition</i>
Module 2	0.94	1.90	0.85	35.0	
Module 3	0.50	1.90	0.44	20.0	

357 a = yield calculated from recovered dry product crystals

358



359

360 **Figure 7.** Crystal size distributions (a) and average crystal size $D[4,3]$ (b) of phthalic acid obtained from
 361 continuous sonicated cooling crystallizer with equal supersaturation ratio in each module with different
 362 supersaturation ratios (different initial temperature) at a residence time of 9.05 mins.

363

364 3.4 Effect of ultrasound

365 For all of the studied experimental conditions without ultrasound, small amount of crystals were
 366 obtained from the crystallization process, which were not enough for analysis. This was because the
 367 residence times were short as shown in **Table 4** and there was no ultrasound to induce nucleation in the
 368 system.¹ With ultrasound, only one experiment had similar problem, of no produced crystal, when a

369 flow rate of 150 ml/min and 12 m pipe were used because of the short residence time which was
370 probably lower than the induction time, hence there was a reduced effect of ultrasound with this
371 operating condition. From **Table 4**, it is observed that the actual yield was always higher for sonicated
372 experiments compared to non-sonicated experiments at a specific residence time. Thus, it indicates that
373 the crystallization process was enhanced significantly by ultrasound. Moreover, encrustation can be
374 avoided by using ultrasound assisted crystallization.³⁷

375 Figure 8 shows the crystal size distributions and average crystal sizes of phthalic acid obtained from
376 cooling sonocrystallization process. The CSDs show wider distributions for lower flow rates (higher
377 residence time) for the 12 m and 18 m pipes, represented in Figure 8a and Figure 8b respectively,
378 compared to the higher flow rates in the experiment. However, the CSDs were not consistent probably
379 due to the effect of ultrasound and the possible relationship between available residence times and
380 induction times of phthalic acid.

381 More so, a sequence of decrease in average crystal size and yield was observed with increase in flow
382 rate as presented in **Table 4** and **Figure 8c** respectively. This was due to the short residence time crystals
383 spent in the crystallizer, not giving enough time for crystals to grow immediately after nucleation
384 induced by ultrasound. Another reason for this is the possibility of the residence time being very close to
385 the induction time which was not studied. Using the 18 m pipe and the flow rate of 150 ml/min without
386 using ultrasound, the yield was unreliable due to temperature variation during the filtration of the
387 product suspension. When the flow rate of 50 ml/min and 18 m pipe were used, the particle size was
388 very similar with the crystals obtained with flow rate of 100 ml/min. This might be due to the
389 classification of crystals in the pipe with such low flow velocity.

390 Interestingly, the yields obtained from ultrasound experiments were higher compared to those
391 without ultrasound, at the same condition as seen in **Table 4**. Since ultrasound can reduce the induction

392 time,^{1,10} hence, nucleation begins earlier for such experiments carried out with ultrasound thereby
 393 offering more yield.

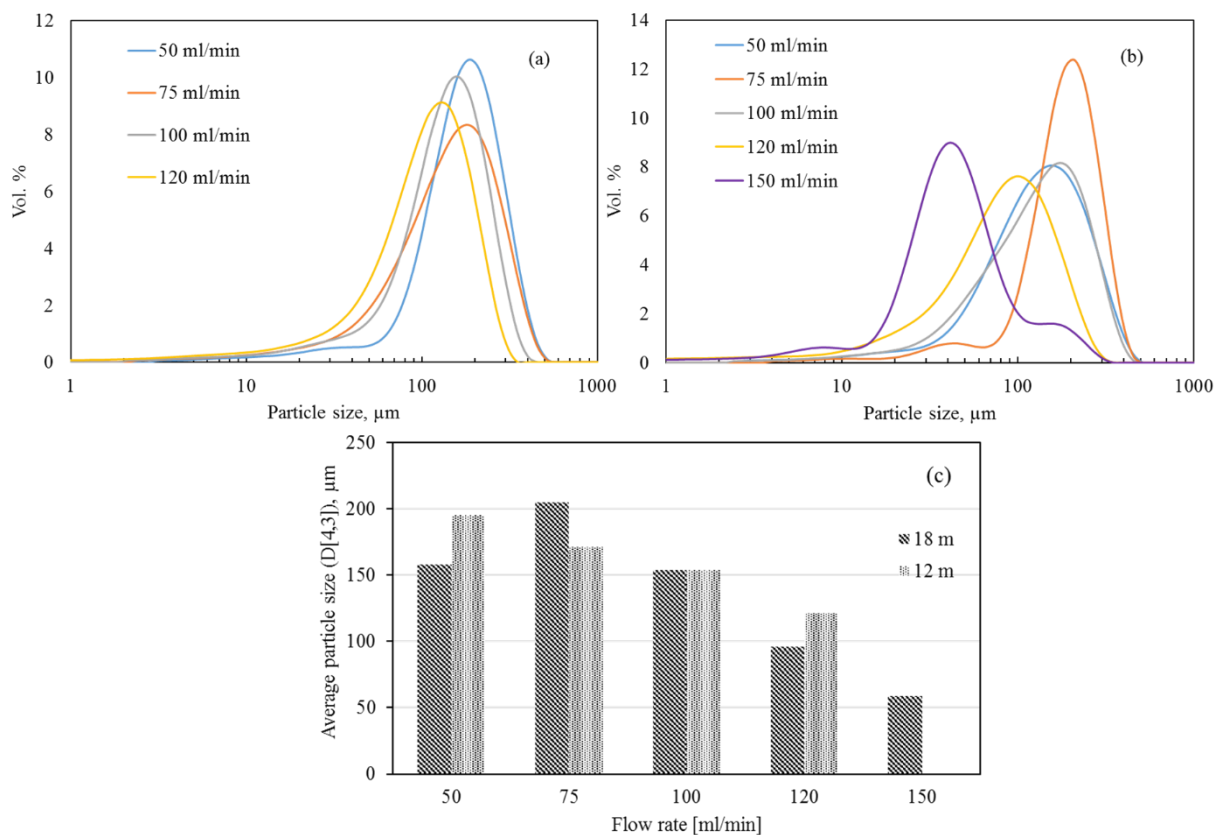
394

395 **Table 4.** Results of phthalic acid samples obtained from cooling crystallization with and without
 396 ultrasound in the one module crystallizer having inner diameter of 4 mm.

Pipe length, m	Ultrasound	Flow rate, ml/min	Residence time, mins	Conc. of mother liquor, g/100g water	Yield ^b , %	
12	ON	50	3.02	0.69	59	
		75	2.01	0.81	31	
		100	1.51	0.78	37	
		120	1.26	0.79	34	
		150	1.01	0.81	31	
	OFF	50	3.02	0.74	47	
		100	1.51	0.83	27	
		150	1.01	0.83	27	
	18	ON	50	4.52	0.71	54
			75	3.02	0.75	45
100			2.26	0.77	39	
120			1.88	0.81	31	
150			1.51	0.81	31	
OFF		50	4.52	0.79	36	
		100	2.26	0.78	37	
		150	1.51	0.76	42*	

397 ^b = yield calculated from mother liquor concentration, * = unreliable.

398



399
 400 **Figure 8.** Crystal size distributions of phthalic acid from 12 m pipe (a) and 18 m pipe (b) and their
 401 average crystal sizes (c), obtained from cooling sonocrystallization process with one module.

402
 403 **4. CONCLUSION**

404 Continuous cooling crystallization of three model compounds (K_2SO_4 , $CuSO_4$ and phthalic acid) were
 405 carried out in a new modular sonicated tubular crystallizer. Feasible conditions were obtained from
 406 successful operating processes running without pipe blockage for three or four times of the residence
 407 time. The residence time is a critical factor for yield and crystal size according to results. The yield is
 408 affected by nucleation and crystallization time which can relate to supersaturation left in the reactor
 409 outlet with short residence times.

410 The cooling strategy did not have a clear relation to the crystal size distributions. This might be due to
 411 the difference of solubilities, crystal growth, nucleation kinetics, and crystal properties for each

412 compound. Equal supersaturation could be used as the best option to design temperature profiles for
413 cooling crystallization. This is because each module would ideally have equal concentration difference
414 and thus leads to moderate local supersaturation which could reduce the opportunity of crystals to
415 block the pipes. More so, equal supersaturation produces higher yields in cases where short residence
416 times are used. This is favoured especially in targeting production increase with continuous systems.
417 Furthermore, the design criteria were evaluated with the studied three model compounds. Ultrasound
418 plays a critical role, which can enhance the crystallization process significantly and avoid clogging. From
419 results, the use of ultrasound offered higher yields compared to experiments without ultrasound.
420 Boundary conditions such as residence time and cooling strategy as the key issues have to be taken into
421 account when designing a continuous tubular sonocrystallizer. As further studies optimization between
422 the process residence time and the supplied ultrasound intensity is needed.

423

424 AUTHOR INFORMATION

425 **Corresponding Author**

426 *E-mail: tuomas.koiranen@lut.fi, Phone number: +358 50 4357414

427 *E-mail: nnaemeka.ezeanowi@lut.fi

428 **Notes**

429 The authors declare no competing financial interest

430 ACKNOWLEDGEMENT

431 The authors thank the Finnish Funding Agency for Technology and Innovation, Tekes, for their financial
432 support. The authors also thank M.Sc. Juhani Pouta for his contribution to the experimental work.

433

434 REFERENCES

- 435 1. Tung, H.; Paul, E.; Midler, M.; McCauley, J. In *Crystallization of Organic Compounds: An*
436 *Industrial perspective*. Hoboken, NJ: John Wiley & Sons, Inc., 2009; Chapter 7, pp. 143-144.
- 437 2. Lawton, S.; Steele, G.; Shering, P.; Zhao, L.; Laird, I.; Ni, X-W. Continuous crystallization of
438 pharmaceuticals using a continuous oscillatory baffled crystallizer. *Org. Process Res. & Dev.*
439 **2009**, 13, 1357-1363.
- 440 3. Hohmann, L.; Gorny, R.; Klaas, O.; Ahlert, J.; Wohlgemuth, K.; Kockmann, N. Design of
441 Continuous tubular cooling crystallizer for process development on lab-scale. *Chem. Eng.*
442 *Technol.* **2016**, 39, 1268-1280.
- 443 4. Zhao, L; Raval, V.; Briggs, N. E. B.; Bhardwaj, R. M.; McGlone, T.; Oswald, I. D. H.; Florence, A. J.
444 From discovery to scale-up: α -lipoic acid: nicotinamide co-crystals in a continuous oscillatory
445 baffled crystalliser. *Cryst. Eng. Comm.* **2014**, 16 (26), 5769-5780.
- 446 5. NiTech® Solutions Limited. Products. Online. 2018; Available at:
447 <http://www.nitechsolutions.co.uk/products>. [Accessed September 25, 2018].
- 448 6. Kacker, R.; Regensburg, S. I.; Kramer, H. J. M. Residence time distribution of dispersed liquid
449 and solid phase in a continuous oscillatory flow baffled crystallizer. *Chem. Eng. J.* **2017**, 317,
450 413-423.
- 451 7. Hohmann, L.; Greinert, T.; Mierka, O.; Turek, S.; Schembecker, G.; Bayraktar, E.; Wohlgemuth,
452 K.; Kockmann, N. Analysis of crystal size dispersion effects in a continuous coiled tubular
453 crystallizer: experiments and modeling. *Cryst. Growth Des.* **2018**, 18, 1459-1473.

- 454 8. Eder, R. J. P.; Radl, S.; Schmitt, E.; Innerhofer, S.; Maier, M.; Gruber-Woelfler, H.; Khinast, J. G.
455 Continuously seeded, continuously operated tubular crystallizer for the production of active
456 pharmaceutical ingredients. *Cryst. Growth Des.* **2010**, 10, 2247-2257.
- 457 9. Kim, H. N.; Suslick, K. S. The effects of ultrasound on crystals: Sonocrystallization and
458 sonofragmentation. *Crystals* **2018**, 8, 280.
- 459 10. Ruecroft, G.; Hipkiss, D.; Ly, T.; Maxted, N.; Cains, P. W. Sonocrystallization: the use of
460 ultrasound for improved industrial crystallization. *Org. Process Res. & Dev.* **2005**, 9, 923-932.
- 461 11. Bang, J. H.; Suslick, K. S. Application of ultrasound to the synthesis of nanostructured
462 materials. *Adv. Mater.* **2010**, 22, 1039-1059.
- 463 12. Li, H. X; Li, H.; Zhang, J.; Dai, W. L.; Qiao, M. H. Ultrasound-assisted preparation of a highly
464 active and selective Co-B amorphous alloy catalyst in uniform spherical nanoparticles. *J. Catal.*
465 **2007**, 246, 301-307.
- 466 13. Zhang, D.; Xu, S.; Du, S.; Wang, J.; Gong, J. Progress of pharmaceutical continuous
467 crystallization. *Engineering*, **2017**, 3, 354-364.
- 468 14. Dhumal, R. S.; Biradar, S. V.; Paradkar, A. R.; York, P. Ultrasound assisted engineering of
469 lactose crystals. *Pharm. Res.* **2008**, 25, 2835-2844.
- 470 15. Arakelyan, V. S. Effect of ultrasound on crystal growth from melt and solution. *Acta Phys.*
471 *Hung.* **1987**, 61, 185-187.
- 472 16. Vancleef, A.; Seurs, S.; Jordens, J.; Van Gerven, T.; Thomassen, L.C.J.; Braeken, L. Reducing the
473 induction time using ultrasound and high-shear mixing in a continuous crystallization process.
474 *Crystals* **2018**, 8, 326.

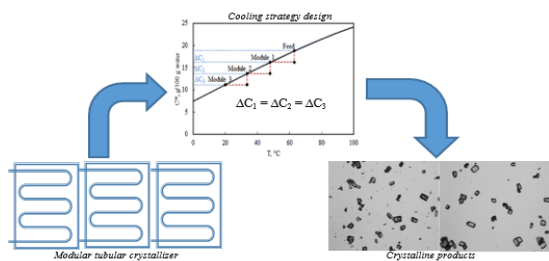
- 475 17. Flowers, B. S.; Hartman, R. L. Particle handling techniques in microchemical processes.
476 *Challenges* **2012**, 3, 194-211.
- 477 18. Hartman, R. L. Managing solids in microreactors for the upstream continuous processing of
478 fine chemicals. *Org. Process Res. Dev.*, **2012**, 16, 870–887.
- 479 19. Rossi, D.; Jamshidi, R.; Saffari, N.; Kuhn, S.; Gavriilidis, A.; Mazzei, L. Continuous-flow
480 sonocrystallization in droplet-based microfluidics. *Cryst. Growth Des.* **2015**, 15, 5519-5529.
- 481 20. Wu, K.; Kuhn, S. Strategies for solids handling in microreactors. *Chim. Oggi* **2014**, 32, 62-66.
- 482 21. Furuta, M.; Mukai, K.; Cork, D.; Mae, K. Continuous crystallization using a sonicated tubular
483 system for controlling particle size in an API manufacturing process. *Chem. Eng. Process.* **2016**,
484 102, 210-218.
- 485 22. Mersmann, A.; Rennie, F. W. In *Crystallization Technology Handbook*; Mersmann, A., Ed.;
486 Second Edition, Marcel Dekker: New York, 2001; Chapter 9, pp. 393-444.
- 487 23. Alvarez, A. J.; Singh, A.; Myerson, A. S. Crystallization of cyclosporine in a multistage
488 continuous MSMPR crystallizer. *Cryst. Growth Des.* **2011**, 11, 4392-4400.
- 489 24. Li, J.; Trout, B. L.; Myerson, A. S. Multistage continuous mixed-suspension, mixed-product
490 removal (MSMPR) crystallization with solids recycle. *Org. Process Res. Dev.* **2016**, 20, 510-516.
- 491 25. Power, G.; Hou, G.; Kamaraju, V. K.; Morris, G.; Zhao, Y.; Glennon, B. Design and optimization
492 of a multistage continuous cooling mixed suspension, mixed product removal crystallizer.
493 *Chem. Eng. Sci.* **2015**, 133, 125-139.

- 494 26. Siddique, H.; Brown, C. J.; Houson, I.; Florence, A. J. Establishment of a continuous
495 sonocrystallization process for lactose in an oscillatory baffled crystallizer. *Org. Process Res.*
496 *Dev.* **2015**, *19*, 1871-1881.
- 497 27. Eder, R. J. P.; Schrank, S.; Besenhard, M. O.; Roblegg, E.; Gruber-Woelfler, H.; Khinast, J. G.
498 Continuous sonocrystallization of acetylsalicylic acid (ASA): control of crystal size. *Cryst.*
499 *Growth Des.* **2012**, *12*, 4733-4738.
- 500 28. Besenhard, M. O.; Neugebauer, P.; Ho, C. D.; Khinast, J. G. Crystal size control in a continuous
501 tubular crystallizer. *Cryst. Growth Des.* **2015**, *15*, 1683-1691.
- 502 29. Ruecroft, G.; Burns, J. An apparatus and process for producing crystals. Patent application:
503 WO 2010/079350 A2, 2010.
- 504 30. Su, Q.; Nagy, Z. K.; Rielly, C. D. Pharmaceutical crystallization processes from batch to
505 continuous operation using MSMR stages: Modelling, design, and control. *Chem. Eng. and*
506 *Process.* **2015**, *89*, 41-53.
- 507 31. Docbrown.info. Gas and Salt Solubility in Water and Solubility Curves. Online, 2000; Available
508 at: <http://www.docbrown.info/page01/AqueousChem/AqueousChem4.htm> [Accessed 6 Jul.
509 2015].
- 510 32. Stephen, H.; Stephen, T., Eds. In *Solubilities of Inorganic and Organic Compounds*; Pergamon
511 Press, 1963; 2nd ed., Vol. 1, Part 1, pp. 438-439.
- 512 33. Linga, Å. In *Effects of Seeding on the Crystallization Behaviour and Filtration Abilities of an*
513 *Aromatic Amine*. Master's thesis: NTNU, 2017; pp 3-90.

- 514 34. Raphael, M.; Rohani, S.; Sosulski, F. Isoelectric precipitation of sunflower protein in a tubular
515 precipitator. *Can. J. Chem. Eng.* **1995**, 73, 470–483.
- 516 35. Hartel, R. W. In *Handbook of Industrial Crystallization*; Myerson, A. S., Ed.; Butterworth-
517 Heinemann: Boston, 2002; Second Edition, Chapter 13, pp. 287-303.
- 518 36. Louhi-Kultanen, M.; Karjalainen, M.; Rantanen, J.; Huhtanen, M.; Kallas, J. Crystallization of
519 glycine with ultrasound. *Int. J. Pharm.* **2006**, 320, 23-29.
- 520 37. Myerson, A. S.; Ginde, R. In *Handbook of Industrial Crystallization*; Myerson, A. S., Ed.;
521 Butterworth-Heinemann: Boston, 2002; Second Edition, Chapter 2, pp. 33-62.
- 522 38. Ni, X.; Liao, A. Effects of Cooling Rate and Solution Concentration on Solution Crystallization of
523 L-Glutamic Acid in an Oscillatory Baffled Crystallizer. *Cryst. Growth Des.* **2008**, 8(8), 2875-2881.
- 524 39. Kaneko, S.; Yamagami, Y.; Tochiara, H.; Hirasawa, I. Effect of Supersaturation on Crystal Size
525 and Number of Crystals Produced in Antisolvent Crystallization. *J. Chem. Eng. Japan* **2002**,
526 35(11), 1219-1223.
- 527 40. Sarig, S.; Eidelman, N.; Glasner, A.; Epstein, J. A. The effect of supersaturation on the crystal
528 characteristics of potassium chloride. *J. appl. Chem. Biotechnol.* **1978**, 28, 663 -667.
- 529

530 **For Table of Contents Use Only**

531 TABLE OF CONTENTS GRAPHIC



532

533

534 SYNOPSIS

535 Process parameters were studied in a continuous sonicated modular cooling crystallizer with inorganic
536 and organic model compounds. Equal supersaturation as a crystallization design strategy allows high
537 yields especially with short processing times. Smaller crystals and higher yields can be obtained using
538 ultrasound in continuous crystallization systems. Residence time is an important design variable of such
539 systems.